BJP BRITISH JOURNAL OF PHARMACOLOGY

BPS BRITISH PHARMACOLOGICAL SOCIETY

British Journal of Pharmacology (2010), 159, 1497–1510

0007-1188/10
www.brjpharmacol.org

RESEARCH PAPER

Andrographolide regulates epidermal growth factor receptor and transferrin receptor trafficking in epidermoid carcinoma (A-431) cells

Y Tan, KH Chiow, D Huang and SH Wong

Laboratory of Membrane Trafficking and Immunoregulation, Department of Microbiology, Immunology Programme, Yong Loo Lin School of Medicine, National University of Singapore, Singapore, Republic of Singapore

Background and purpose: Andrographolide is the active component of *Andrographis paniculata*, a plant used in both Indian and Chinese traditional medicine, and it has been demonstrated to induce apoptosis in different cancer cell lines. However, not much is known about how it may affect the key receptors implicated in cancer. Knowledge of how andrographolide affects receptor trafficking will allow us to better understand new mechanisms by which andrographolide may cause death in cancer cells.
Experimental approach: We utilized the well-characterized epidermal growth factor receptor (EGFR) and transferrin receptor (TfR) expressed in epidermoid carcinoma (A-431) cells as a model to study the effect of andrographolide on receptor trafficking. Receptor distribution, the total number of receptors and surface receptors were analysed by immunofluorescence, Western blot as well as flow-cytometry respectively.
Key results: Andrographolide treatment inhibited cell growth, down-regulated EGFRs on the cell surface and affected the degradation of EGFRs and TfRs. The EGFR was internalized into the cell at an increased rate, and accumulated in a compartment that co-localizes with the lysosomal-associated membrane protein in the late endosomes.
Conclusion and implications: This study sheds light on how andrographolide may affect receptor trafficking by inhibiting receptor movement from the late endosomes to lysosomes. The down-regulation of EGFR from the cell surface also indicates a new mechanism by which andrographolide may induce cancer cell death.
British Journal of Pharmacology (2010) **159,** 1497–1510; doi:10.1111/j.1476-5381.2009.00627.x; published online 3 March 2010

Keywords: andrographolide; epidermal growth factor receptor; transferrin receptor

Abbreviations: ADO, andrographolide; EGF, epidermal growth factor; EGFR, epidermal growth factor receptor; LAMP-1, lysosomal-associated membrane protein-1; TfR, transferrin receptor; VAMP, vesicle-associated membrane protein

Introduction

Andrographolide (ADO) is the main active constituent of the plant *Andrographis paniculata*. It is a widely used herb in traditional Chinese medicine, Ayurvedic medicine and is a key constituent of the Scandinavian herbal concoction Kan Jang. This versatile compound has been found to have hepatoprotective effects against toxic substances (Sheeja and Kuttan, 2006), and it also has anti-inflammatory properties, as it can suppress inflammation by inhibiting the nuclear translocation of NF-κB (Singha *et al.*, 2007; Bao *et al.*, 2009). It has also been demonstrated to be an anticancer compound, as it can cause apoptosis of hepatocellular carcinoma cells (Yang *et al.*, 2009b), as well as induce cell cycle arrest in colorectal carcinoma cells (Shi *et al.*, 2008). Furthermore, andrographolide affects dendritic cell maturation by inhibiting the up-regulation of I-A^b, CD40 and CD86 after lipopolysaccharide induction of dendritic cells (Iruretagoyena *et al.*, 2005). This suggested that andrographolide may have an effect on the trafficking of these molecules to the cell surface, and thus we hypothesized that its anti-neoplastic effect could be due to its ability to regulate the cell surface expression and trafficking of growth-regulating receptors, such as the epidermal growth factor receptor (EGFR) and the transferrin receptor (TfR). These two receptors are of interest as both are known to be up-regulated in cancers. In particular, EGFR has been shown to be up-regulated in various cancers involving the

Correspondence: Siew Heng Wong, Laboratory of Membrane Trafficking and Immunoregulation, Department of Microbiology, Immunology Programme, Yong Loo Lin School of Medicine, National University of Singapore, Singapore 117597, Republic of Singapore. E-mail: micwsh@nus.edu.sg
Received 21 May 2009; revised 2 November 2009; accepted 19 November 2009

head and neck (Gold *et al*., 2009), lung (Dy and Adjei, 2009), gliomas (Kesari *et al*., 2006) and ovaries (Lafky *et al*., 2008); while TfR is known to be overexpressed in breast cancer (Habashy *et al*., 2010). As such, EGFR and TfR have become prime targets in the development of cancer therapies (Lepelletier *et al*., 2007; Capdevila *et al*., 2009), and hence, they are also the focus of our current study. In addition, these two receptors follow different pathways upon internalization into the cell. Hence, discerning the effects of andrographolide on these two receptors would be useful in the detection of how it may differentially affect trafficking of these receptors within the cell. Furthermore, the trafficking of these receptors has been studied extensively, making it much easier to establish the membrane compartments which andrographolide affects.

Epidermal growth factor receptor is a well-characterized key transmembrane receptor involved in signalling pathways for cell growth. In its inactive state, it is known to localize on the plasma membrane to cholesterol-rich lipid rafts, which are detergent-resistant regions that are distinct from caveolae (Pike, 2005). Upon the binding of EGF to EGFR, the tyrosine kinase receptors dimerize and autophosphorylate, forming the active state, which triggers the Ras-mitogen-associated protein kinase (MAPK) pathway for cell proliferation. The receptors are then internalized into the cells for down-regulation. In the classical clathrin-dependent endocytic pathway, EGFR moves out of the lipid rafts into clathrin-coated pits after the dimerization and phosphorylation of the receptors. Cbl, a ubiquitin E3 ligase, then binds and ubiquitinates the receptors and the proteins associated with EGFR, epsin and EPS15 (Le Roy and Wrana, 2005). Upon entry into the cell, the receptor moves to the early endosomes and is either recycled back up to the cell surface, or moved to the multivesicular body (MVB) where it will be transported via the endosomal sorting complex required for transport (ESCRT) to the late endosomes and lysosomes for degradation.

TfR is a 95 kDa transmembrane receptor that is important for the uptake of iron (Daniels *et al*., 2006). TfR binds transferrin, which binds to two ferric ions, and like EGFR, is endocytosed in clathrin-coated pits. It then moves to the sorting endosomes, where the iron ions are released due to the lower pH of the endosomes, to the endocytic recycling compartment, and back to the plasma membrane (Maxfield and McGraw, 2004).

The aim of this study was to elucidate the effects of andrographolide on receptors critical for the proliferation and survival of the human epidermoid carcinoma A-431 cells. A-431 cells were chosen as it is a cancer cell line, and expresses our receptors of interest, EGFR (Wrann and Fox, 1979) and TfR (Hopkins and Trowbridge, 1983), at high levels. In this study, we showed that andrographolide causes the down-regulation of EGFR from the cell surface as well as the inhibition of EGFR and TfR degradation.

Methods

Cell culture, reagents and drug treatments

A-431 human skin epithelial carcinoma cells (CRL-1555) were obtained from ATCC, and cultured in DMEM supplemented with 5% foetal bovine serum (FBS), 2 mM L-glutamine, 0.1 mM non-essential amino acids, 5 mM HEPES buffer and 1X antibiotic-antimycotic (Gibco, Singapore). The cell culture was routinely grown at 37°C with 5% CO_2. Andrographolide was resuspended in dimethyl sulphoxide (DMSO), to give a stock concentration of 50 mM and stored at –20°C. DMSO was utilized as a vehicle control in all experiments involving andrographolide, and the amount of DMSO used was standardized across different concentrations of andrographolide. Unconjugated epidermal growth factor (EGF) and Alexa Fluor 555 labelled EGF were reconstituted in sterile water and stored at –20°C.

Cytotoxicity assay

Cell viability was assessed by MTT (3-(4,5-dimethylthiazol-2-yl)-2,5-diphenyltetrazolium bromide) as previously described (Li *et al*., 2007; Pannecouque *et al*., 2008). Briefly, cells were seeded into a 96-well microplate and routinely cultured. Cells were then exposed to andrographolide (0–160 μM) for 24 h. The amount of DMSO (1% v/v) in each well was standardized across all samples; 20 μL of tetrazolium dye solution (5 mg·mL^{-1} in phosphate buffered saline, PBS) was added to each well and incubated for 1 h with shaking in the dark. Cells were then lysed overnight in the presence of lysis buffer at 37°C to dissolve the formazan crystals. The absorbance was then read using a microplate reader (Tecan Gemini Infinite 200) at 540 nm, and with reference filter at 690 nm to deduct for absorbance due to cell debris.

Quantification of surface receptors

Cells were pretreated with DMSO (0.2% v/v) or andrographolide, and harvested in 2 mM EDTA. Cells were then blocked and probed with primary antibodies, washed, and probed with secondary antibodies. Cells were then fixed with 2% paraformaldehyde and analysed using the Cytomics FC 500 Series Flow Cytometry Systems (Beckman Coulter). Antibodies used were clone LA1 mouse anti-EGFR antibody and mouse IgG1 Isotype Control.

Western blot analysis

Cells were pretreated with DMSO (0.2% v/v) or andrographolide for 4 h, and harvested by 2 mM EDTA and lysed for an hour using 1% Triton X-100 supplemented with 2x complete protease inhibitor cocktail and 2 mM phenylmethanesulphonylfluoride in PBS. Protein concentration was read using the Bradford assay, resolved on an SDS-PAGE gel and transferred to a nitrocellulose membrane. Blots were then blocked with 5% skimmed milk in PBS and 0.1% Tween-20 and probed using the primary antibodies and secondary antibodies in blocking buffer. The secondary antibodies used were anti mouse or rabbit conjugated horse radish peroxidase IgG antibodies. The immunoreactive bands were visualized using chemiluminescent substrate (Thermo Scientific, Rockford, IL, USA) and exposed to X-ray film (Thermo Scientific, Rockford, IL, USA). The resulting blot was then scanned and quantified using ImageJ and normalized. The primary antibodies used

were: anti-EGFR (Clone F4), anti-β-actin and anti-activated EGFR.

RNA extraction and reverse transcription-polymerase chain reaction (RT-PCR)

Cells were pretreated with DMSO (0.2% v/v) or andrographolide for 4 h. Total RNA was extracted using TRIzol reagent following the manufacturer's instructions. First strand synthesis was performed using 7 μg of total RNA, oligo dT primer and M-MLV Reverse Transcriptase following the manufacturer's instructions and polymerase chain reaction (PCR) performed using the GeneAmp PCR System 9700. The corresponding PCR product was then analysed by agarose gel electrophoresis.

Primers: EGFR forward primer 5′-ATGCAAATAAAACCG GACTGAAGG-3′; EGFR reverse primer 5′-ACGTGGTGGG GTTGTAGAGCA-3′; β-actin forward primer 5′-GAACCCTA AGGCCAACCGTGAAAAGATG-3′; β-actin reverse primer 5′-GGCCAGCCAAGTCCAGACGCAG-3′.

Indirect immunofluorescence

Immunofluorescence microscopy was performed as described previously (Wong *et al.*, 1998; 1999). Briefly, cells grown on coverslips were treated for 4 h with DMSO (0.2% v/v) or andrographolide and fixed in 4% paraformaldehyde on ice. After being fixed, the cells were then made permeable with 0.1% saponin, and stained with the corresponding primary antibodies and secondary fluorescence-conjugated antibodies. The coverslips were mounted using fluorescence mounting medium. Conventional images were taken with the fluorescent microscope (Olympus BX60).

Immunofluorescence kinetics assay

Cells were serum starved when labelled epidermal growth factor (EGF) was used in the experiment. The cells were pretreated with DMSO (0.2% v/v) or andrographolide for 30 min, and incubated with mouse antibody EGFR (Clone 29.1) or 1.6 $\mu g \cdot mL^{-1}$ Alexa Fluor 555-labelled EGF for 1 h on ice, to allow the antibody or ligand to bind to cell surface receptors. Cells were then replaced into media containing DMSO (0.2% v/v) or andrographolide, washed and fixed at the appropriate time points, then stained and mounted in the manner stated above. Confocal microscopy was carried out using the Olympus FV500 confocal microscope, and images obtained were processed using the Olympus Fluoview software.

Western blot kinetics analysis

Cells were incubated on ice with anti-EGFR (Clone 29.1) (Kodama *et al.*, 1995) or anti-TfR (OKT9, monoclonal hybridoma) (Goding and Burns, 1981) for 1 h, and were then placed in complete media with DMSO (0.2% v/v) or andrographolide, incubated at 37°C in the CO_2 incubator for various time points, detached from the plate using 2 mM EDTA and then lysed. The lysate was then separated on a SDS-PAGE gel and transferred onto a nitrocellulose membrane. The blots were then blocked with 5% skimmed milk in PBS and 0.1% Tween-20 and probed using the appropriate horse radish peroxidize conjugated secondary antibody.

Transferrin recycling assay

Cells were pretreated with DMSO (0.2% v/v) or andrographolide and starved in serum free-DMEM for 4 h. Cells were then incubated with Alexa Fluor 488 conjugated transferrin for 1 h at 17°C in the presence of the compound to allow transferrin to be trapped in the recycling compartment. Residual surface transferrin was then washed off with ice-cold acid wash (pH 3.5) and the cells were then washed with DMEM and PBS. Cells were then placed in the CO_2 incubator in PBS, with holo-transferrin and either DMSO or andrographolide, to allow for the trapped transferrin to be recycled. PBS was collected at selected time points and the cells in the dish lysed. The amount of fluorescent transferrin in the PBS and cell lysates was quantified using the microplate reader (Tecan Gemini Infinite 200) using an excitation wavelength of 480 nm and emission wavelength of 520 nm. The percentage of intracellular transferrin was calculated by the following formula: fluorescence from lysate/(fluorescence from lysate + fluorescence from PBS) × 100.

Receptor internalization assay

Cells were first pretreated with DMSO (0.2% v/v) or andrographolide for 4 h, detached from the plate using 2 mM EDTA, and then stained with anti-EGFR (Clone 29.1) or OKT9 on ice for 1 h. The cells were then washed and placed in complete media with DMSO or andrographolide and incubated at 37°C. At the appropriate time points, the surface bound antibody remaining was washed off cells with an acid wash (pH 2.0). The cells were then fixed with methanol, stained with anti-mouse FITC and analysed using the Cytomics FC 500 Series Flow Cytometry Systems (Beckman Coulter). The percentage of internalized EGFR was calculated by the following formula: fluorescence from intracellular EGFR/(fluorescence from total EGFR) × 100.

EGFR activation assay

Cells were deprived of serum overnight and either incubated in the presence or absence of andrographolide for 4 h, or induced with 50 nM or 100 nM EGF for 15 min. All the cells were then detached from the plate with 2 mM EDTA and lysed. The lysate was then run on a SDS-PAGE gel and transferred onto a nitrocellulose membrane. The blots were then blocked with 5% skimmed milk in PBS and 0.1% Tween-20 and probed using the mouse anti-activated EGFR antibody and the appropriate horse radish peroxidize conjugated secondary antibody.

Statistical analysis

Student's *t*-test was performed for statistical analyses.

Materials

DMEM, FBS, L-glutamine, non-essential amino acids, HEPES and 1X antibiotic-antimycotic for A-431 were all obtained

from Gibco (Singapore). Andrographolide was from Calbiochem (San Diego, CA, USA); DMSO, saponin and MTT were from Sigma (Singapore); EGF from Roche (Indianapolis, IN, USA); Alexa Fluor 555 labelled EGF and Alexa Fluor 488 conjugated transferrin were from Invitrogen (Singapore). The clone LA1 mouse anti-EGFR antibody was obtained from Millipore (Singapore) and the mouse IgG1 Isotype Control from BD Bioscience (San Jose, CA, USA). Primary antibodies: anti-EGFR (Clone F4) and anti-β-actin were from Sigma; anti-activated EGFR from BD Bioscience (San Jose, CA, USA); secondary fluorescence-conjugated antibodies were from Jackson Immunoresearch (West Grove, PA, USA); mouse EGFR antibody (Clone 29.1) was from Sigma; anti-mouse FITC from Jackson ImmunoResearch. The complete protease inhibitor cocktail was from Roche (Indianapolis, IN, USA); the Bradford assay and nitrocellulose membrane from Bio-Rad (Singapore); TRIzol reagent from Invitrogen; M-MLV Reverse Transcriptase from Promega (Singapore); the GeneAmp PCR System 9700 from Applied Biosystems (Singapore); fluorescence mounting medium from Vector Laboratories (Burlingame, CA, USA); EGF from Roche (Indianapolis, IN, USA).

Nomenclature

The nomenclature for the receptors used in this paper is with reference to the 2008 British Journal of Pharmacology's Guide to Receptors and Channels (Alexander *et al.*, 2008).

Results

Andrographolide inhibited growth and down-regulated surface EGFR in A-431 cells

In order to understand the effect of andrographolide on cell proliferation, A-431 cells were exposed to various concentrations of andrographolide for 24 h and analysed by the MTT cytotoxicity assay. As expected from previous work on several other cancer cell lines such as colon cancer (Rajagopal *et al.*, 2003; Kumar *et al.*, 2004), prostate cancer (Kim *et al.*, 2005), liver cancer (Li *et al.*, 2007), leukaemia (Cheung *et al.*, 2005), cervical cancer (Zhou *et al.*, 2006), and promyelocytic leukaemia cells (Manikam and Stanslas, 2009), andrographolide inhibited cancer cell growth. The growth of A-431 cells was inhibited significantly by concentrations of andrographolide from 60 μM onwards (Figure 1A). As EGFR is known to be one of the receptors important for cell growth and proliferation of cancer cells, we went on to investigate whether surface levels of EGFR were affected by andrographolide at concentrations and incubation times that are not known to cause apoptosis. This was to ensure that the observed effects of andrographolide on EGFR were specific to andrographolide, and were not due to downstream events from apoptosis. Approximately 30% of surface EGFRs were found to be down-regulated after andrographolide treatment at both 50 μM and 100 μM (Figure 1B). Interestingly, the down-regulation of EGFR was not dose-dependent. Similarly, down-regulation of approximately 30% of surface EGFR also occurred after treatment of A-431 with concentrations of 5 μM and 15 μM andrographolide for 48 h (Figure 1C). As surface EGFRs were down-regulated by andrographolide, it was possible that andrographolide could have decreased the total number of EGFRs in A-431 cells. However, as shown in A-431 cells treated with andrographolide for 4 h and analysed by Western blot (Figure 1D), the total number of EGFRs was not decreased, but significantly increased by around 15% upon treatment with 100 μM andrographolide. In order to ascertain if the change in total number of EGFRs was due to an increase in EGFR mRNA transcripts, total RNA was extracted from cells treated with 50 μM and 100 μM andrographolide for 4 h and analysed by RT-PCR. From the results, it was evident that there was no change in the amount of EGFR mRNA at the transcriptional level (Figure 1E).

Andrographolide changed the rate of degradation of both EGFR and TfR

As the andrographolide-induced up-regulation of EGFR was not due to an increase in EGFR mRNA transcripts, it is possible that andrographolide regulates trafficking of EGFRs to the lysosomes for degradation in A-431 cells. To determine whether this occurs, surface EGFRs of A-431 cells were labelled with mouse EGFR-specific monoclonal antibody and internalized into the cell at various time points either in the presence or absence of andrographolide. Cells were then lysed and analysed by Western blot using horse radish peroxidase-conjugated anti-mouse antibodies to detect the heavy and light chain of the EGFR-specific antibodies. The degradation rate of the EGFR-specific antibodies was used as a marker for determining the rate of EGFR trafficking to the late lysosomes for degradation. Significant changes in the degradation rate upon andrographolide treatment were observed at 3 and 4 h (Figure 2A, a, lanes 4–7, and b), and the inhibition of the degradation was approximately 22%. Thus, andrographolide delayed trafficking of EGFRs from the cell surface to the lysosomes for degradation. To ascertain whether this inhibition of degradation was specific for EGFR or if it affects general receptor trafficking from the cell surface, a similar degradation assay for TfR was run with anti-TfR antibody. Interestingly, TfR degradation was inhibited significantly at 4 h and up to approximately 47% at 6 h (Figure 2B, a, lanes 4–7, and b). Thus, our results indicate that andrographolide induces the accumulation of both EGFRs and TfRs in intracellular membrane compartments of A-431 cells.

Andrographolide induced the accumulation of EGFRs into an intracellular LAMP-1- and VAMP-8-positive but VAMP-3-negative membrane compartment

The intracellular localization of cell surface internalized EGFRs and TfRs in A-431 cells upon andrographolide treatment was examined by immunofluorescence microscopy. A-431 cells were treated with andrographolide for 4 h, fixed and then stained for EGFR. As can be seen, EGFRs accumulated in compact membrane structures in the perinuclear region, and this effect was slightly more marked after treatment with 100 μM andrographolide (Figure 3A, c). After the addition of EGF, which was utilized to drive the surface EGFRs into the cell, the andrographolide-induced accumulation of EGFRs became more pronounced in comparison with the vehicle control (Figure 3A, e and f). Similarly, internalized

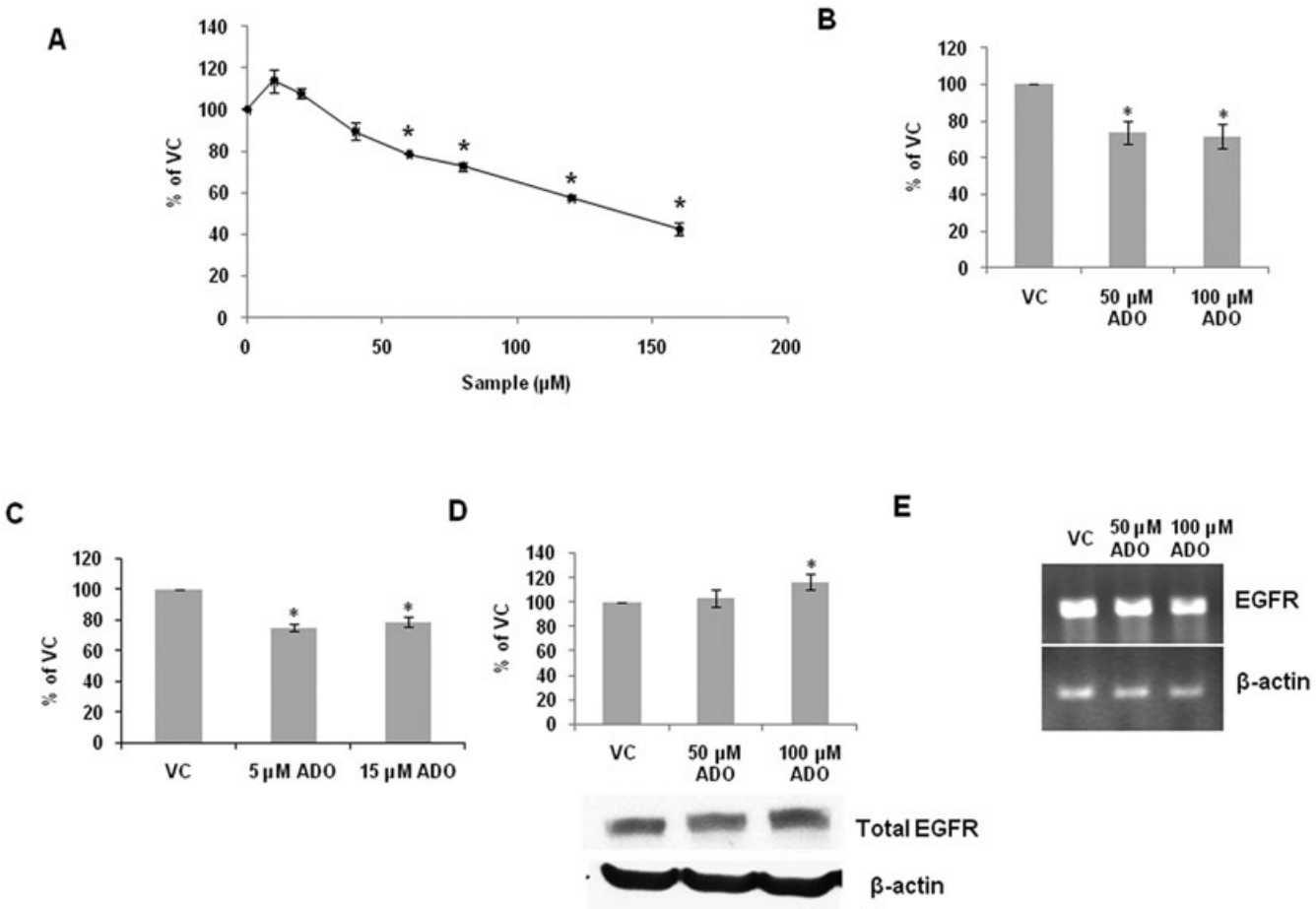

Figure 1 Andrographolide (ADO) inhibits growth and down-regulates surface EGFR in A-431 cells. (A) Assessment of cell viability upon ADO treatment. A-431 cells were treated with various concentrations of ADO for 24 h, and cell viability was assessed by MTT assay. Absorbance values from each concentration were compared with the untreated cells and expressed as a percentage of untreated cells ± SD from two independent experiments. *$P < 0.05$. (B) Surface expression of EGFR after ADO treatment. A-431 cells were treated with various concentrations of ADO for 4 h and then analysed by flow cytometry for surface EGFR. Mean fluorescence intensity of surface receptor levels is expressed as a percentage of vehicle control (VC) ± SD of at least two experiments. *$P < 0.03$. (C) Surface expression of EGFR after 48 h of ADO treatment. A-431 cells were treated with various concentrations of ADO for 48 h and then analysed by flow cytometry for surface EGFR. Mean fluorescence intensity of surface receptor levels was expressed as a percentage of VC, ±SD of at least two experiments. *$P < 0.01$. (D) Western blot analysis of ADO effect on total EGFRs in A-431. A-431 cells were treated with various concentrations of ADO for 4 h and then analysed by Western blot for total EGFRs. Blots are representative of at least two experiments. Intensity of Western blot bands were quantified and normalized to β-actin, then expressed as a percentage of VC ± SD of at least two experiments. *$P < 0.002$. (E) Reverse-transcription polymerase chain reaction (RT-PCR) of EGFR mRNA transcripts. A-431 cells were treated with various concentrations of ADO for 4 h and analysed by RT-PCR. Results are representative of two experiments. EGFR, epidermal growth factor receptor.

surface EGFRs also accumulated at the perinuclear region after treatment with 5 μM and 10 μM andrographolide for 28 h (Figure 3B). To confirm that the EGFRs accumulated in the compact structures originated from the cell surface and not from newly synthesized EGFRs retained in intracellular compartments, such as the Golgi, surface EGFRs of A-431 cells were labelled with anti-EGFR antibody, internalized into the cell after various incubation times in the absence or presence of andrographolide, fixed and analysed by immunofluorescence microscopy. As anticipated, the perinuclear compact membrane structure (PCM) was also apparent (Figure 3C), thus showing that the EGFRs accumulated at the perinuclear compact structure in the presence of andrographolide were EGFRs internalized from the cell surface.

Co-localization studies were then carried out to determine the compartment that EGFRs accumulated in. Under steady-state conditions, where A-431 cells were treated with andrographolide for 4 h and then fixed and stained for EGFR together with a compartmental marker, EGFR did not co-localize well with the vesicle-associated membrane protein-3 (VAMP-3) in cells treated with andrographolide without (Figure 3D, a–i) and with EGF (Figure 3D, j–r). Even though there was some overlap in EGFR and VAMP-3 antibody staining, the shape of the structures staining for VAMP-3 and the andrographolide-induced EGFR clump was different. Confocal 3D convolution and XZ/YZ projection imaging further confirmed that EGFRs and VAMP-3 did not co-localize in the PCM structures (Figure S1). VAMP-3 is a soluble NSF attachment receptor (SNARE) that resides within the early and recycling endosomes (Hong, 2005). EGFRs co-localized better with vesicle-associated membrane protein-8 (VAMP-8) (Figure 3E), a SNARE that resides in both the early and late

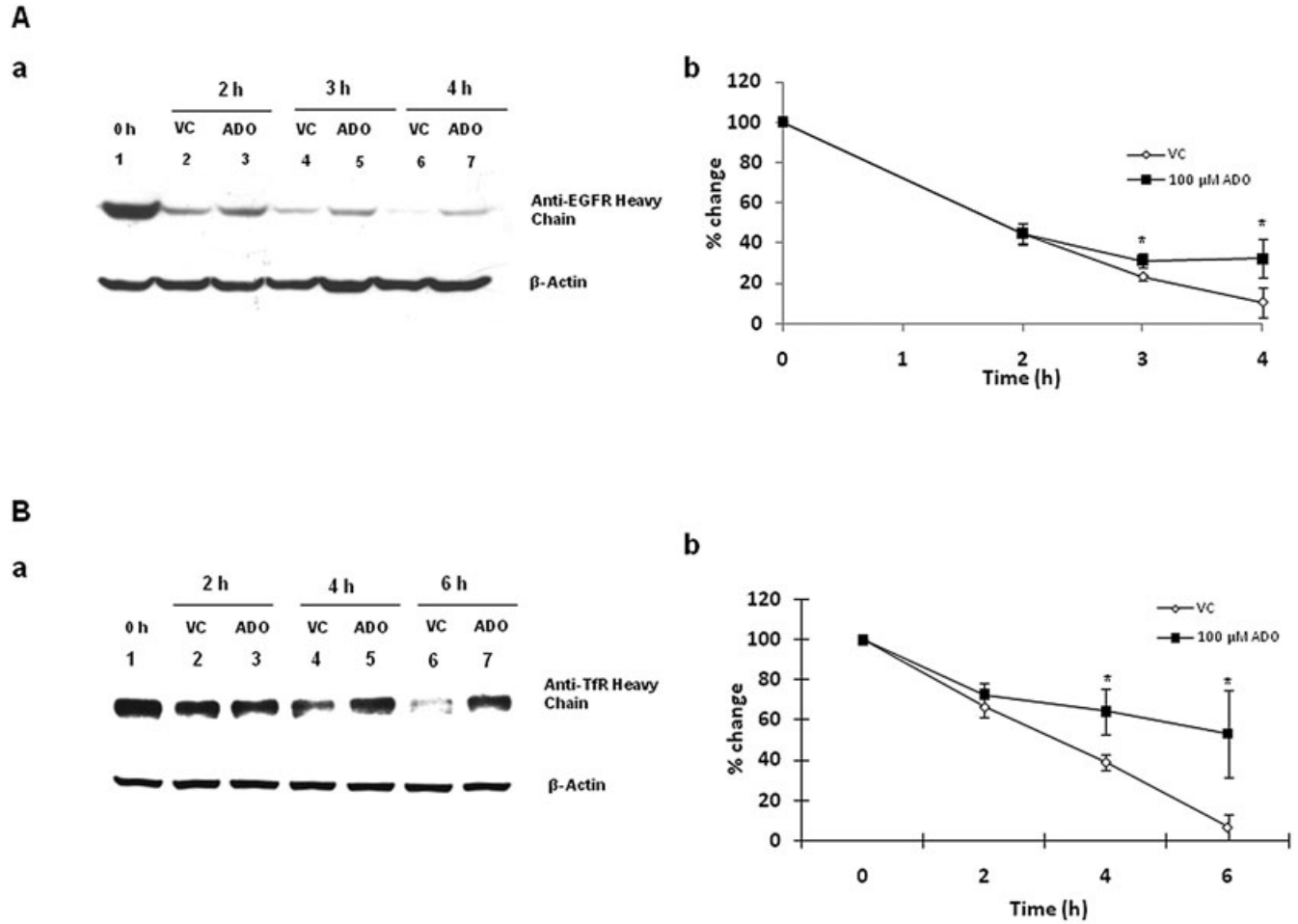

Figure 2 Andrographolide (ADO) changed the rate of degradation of both EGFR and TfR. A-431 cells were incubated with primary antibody on ice for 1 h, treated with DMSO or ADO for the various time points at 37°C and then subjected to Western blot analysis for IgG; β-actin was used as a loading control. Blots are representative of at least three experiments. The intensity of the Western blot bands were quantified and normalized to β-actin, and expressed as a percentage of the initial amount of antibody at 0 h ± SD of at least two experiments (A and B). (A) Internalized EGFR was degraded more slowly in ADO-treated cells. (a) Western blot of internalized EGFR. (b) Quantification of degraded internalized EGFR. *$P < 0.05$. (B) Internalized TfR accumulated in ADO-treated cells although degradation is not inhibited. (a) Western blot of internalized TfR. (b) Quantification of degraded internalized TfR. *$P < 0.03$. EGFR, epidermal growth factor receptor; TfR, transferrin receptor; VC, vehicle control.

endosomes (Wong *et al*., 1998; Antonin *et al*., 2000) in A-431 cells. As can be seen, EGFRs in both the vehicle control and andrographolide-treated cells have structures that are similar to VAMP-8.

Similar results were also obtained for TfR. A-431 cells treated with andrographolide for 4 h, which were then fixed and stained for TfR, showed that TfRs accumulated at the perinuclear compact membrane (PCM) structures (Figure 4A, c). Similarly, TfRs formed a clump under steady-state conditions after treatment with 5 μM or 10 μM andrographolide for 24 h (Figure 4B, b and c). Internalized surface TfRs (labelled with anti-TfR antibody) were also found to accumulate at the perinuclear region after andrographolide-treatment (Figure 4C, d and f). Under steady-state conditions for 4 h, in cells treated with andrographolide, fixed and stained for TfR, and endosomal markers (VAMP-3, and VAMP-8), we observed that TfRs co-localized well with VAMP-8 (Figure 4E), but not VAMP-3 (Figure 4D), in the PCM structures.

In order to further characterize the compartment in which EGFRs are present after andrographolide treatment, surface EGFRs of A-431 cells were labelled with Alexa-conjugated EGF, internalized, fixed at various time points and then co-localized with lysosomal-associated membrane protein-1 (LAMP-1), a commonly used marker for late endosomes and lysosomes (Eskelinen *et al*., 2003). As can be seen, EGFRs were present in the PCM structures in andrographolide-treated cells at the 2 and 4 h time points (Figure 5A, j and p). This result is consistent with the earlier finding that the degradation of EGFRs was inhibited by andrographolide treatment (Figure 2A). Internalized EGF also co-localized well with LAMP-1 after treatment with andrographolide for 2 or 4 h (Figure 5A, l and r). Furthermore, confocal 3D convolution and XZ/YZ projection imaging showed that co-localization of EGF with LAMP-1 in the PCM structures occurred both for the vehicle control (though to a lesser extent) and andrographolide-treated cells (Figure 5B,C). This is not surprising as it is known that the EGFR traffics to the late endosomes and lysosomes for degradation (Le Roy and Wrana, 2005). Hence, this demonstrates that andrographolide induces the accumulation of EGFRs in the late endosomes and lysosomes.

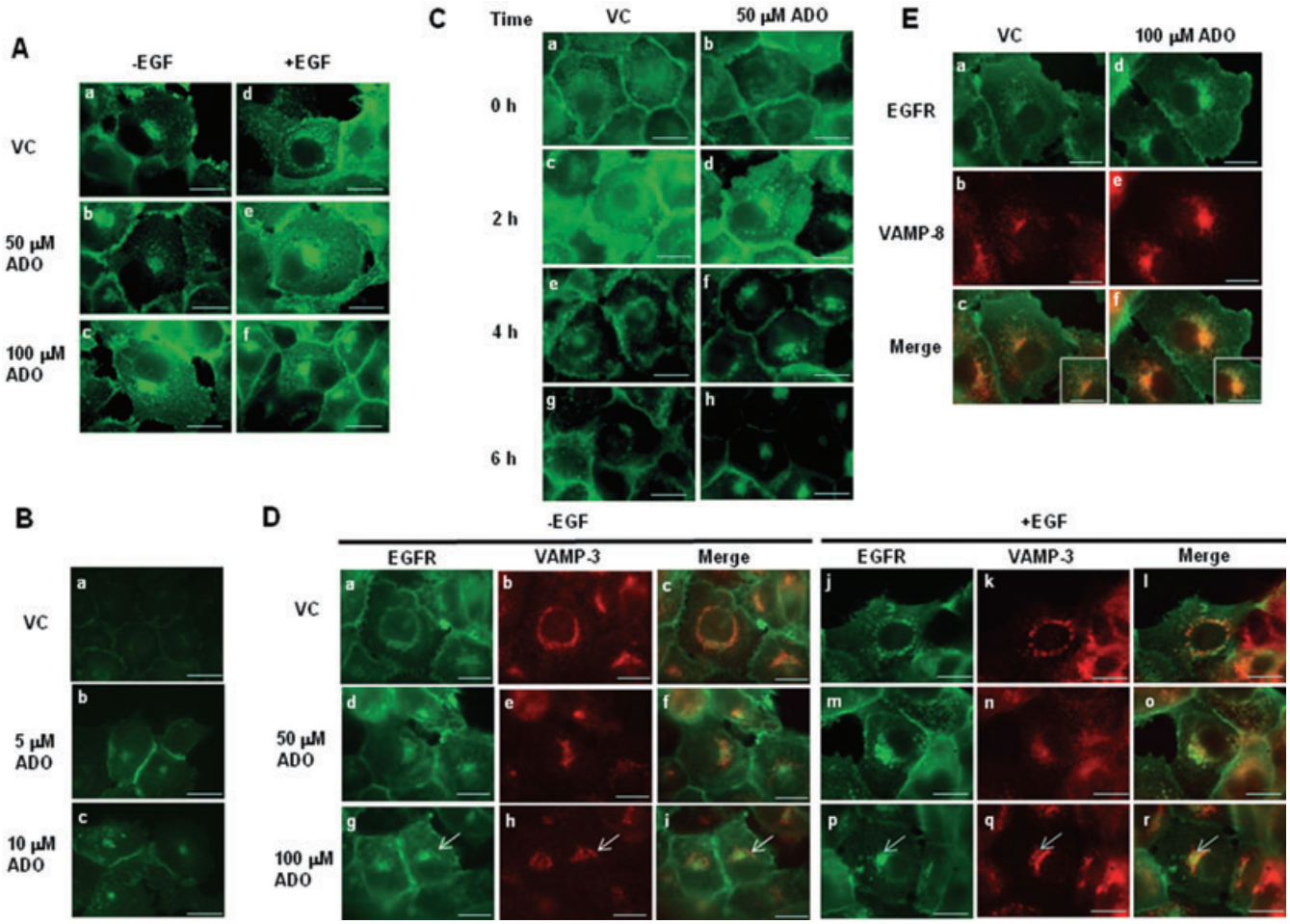

Figure 3 Andrographolide (ADO) affected the intracellular distribution of EGFRs. A-431 cells were treated with various concentrations of ADO for the time points indicated, then fixed and stained with antibodies (A); or treated with various concentrations of ADO for 24 h, incubated with primary antibody on ice, treated with various concentrations of ADO for 4 h at 37°C, and then fixed and stained (B); or they were incubated with primary antibody on ice, and then treated with various concentrations of ADO at 37°C, fixed and stained (C, D, E). Primary antibodies used were against EGFR (monoclonal), VAMP-3 (polyclonal), and VAMP-8 (polyclonal), and secondary antibodies were FITC-conjugated anti-mouse IgG and Cy-3 conjugated anti-rabbit IgG. EGF was utilized to drive the receptors into the cell (A and C, D). Photomicrographs are representative of at least two independent experiments, and were taken with the Olympus BX60 (A–E) at 100× magnification. Scale bars represent 10 μm. (A) Effect of andrographolide on steady-state EGFRs, with and without EGF. (B) Effect of andrographolide on EGFRs internalized from the cell surface for 4 h after 24 h treatment. (C) Effect of andrographolide on EGFRs internalized from the cell surface. The time points tested were 2 h, 4 h and 6 h. (D) The perinuclear clump of EGFRs did not co-localize well with VAMP-3, with and without EGF. (E) The perinuclear clump of EGFRs co-localized well with VAMP-8. Inset image shows enlarged image of EGFR, VAMP-8 co-localization. EGFR, epidermal growth factor receptor; VAMP, vesicle-associated membrane protein; VC, vehicle control.

Down-regulation of surface EGFRs upon andrographolide treatment was not due to the inhibition of receptor recycling but induced by the enhanced internalization of EGFRs from the cell surface of A-431 cells

In view of our observation that andrographolide down-regulates expression of cell surface EGFRs and induces the accumulation of EGFRs in intracellular membrane compartments, there is a possibility that andrographolide could also regulate recycling of EGFRs to the cell surface in A-431 cells. The recycling pathway is responsible for recycling receptors from the endocytic recycling compartment back to the cell surface (Maxfield and McGraw, 2004), and therefore inhibition of this pathway could act as a contributing factor to the inhibition in degradation of both EGFRs and TfRs. To examine this possibility, cells were deprived of serum and either untreated or pretreated with andrographolide for 4 h. Cells were then incubated with labelled transferrin for 1 h, washed and then further incubated for various time points prior to media collection and quantification of recycled labelled transferrin. TfR was utilized here as a marker for the recycling pathway as it is constitutively recycled back to the cell surface. As can be seen, andrographolide did not significantly affect the recycling of TfRs (Figure 6A, a) after incubation times of 0–90 min.

It was also possible that the change in the level of cell surface EGFRs was due to a change in the rate of receptor internalization into the cell. Hence, the rate of receptor internalization was quantified by incubating cells with andrographolide for 4 h. Cell surface receptors were then incubated with anti-EGFR antibody for an hour on ice. Anti-EGFR antibody was then allowed to internalize by incubating the cells in media at 37°C. At each time point, the cells were washed

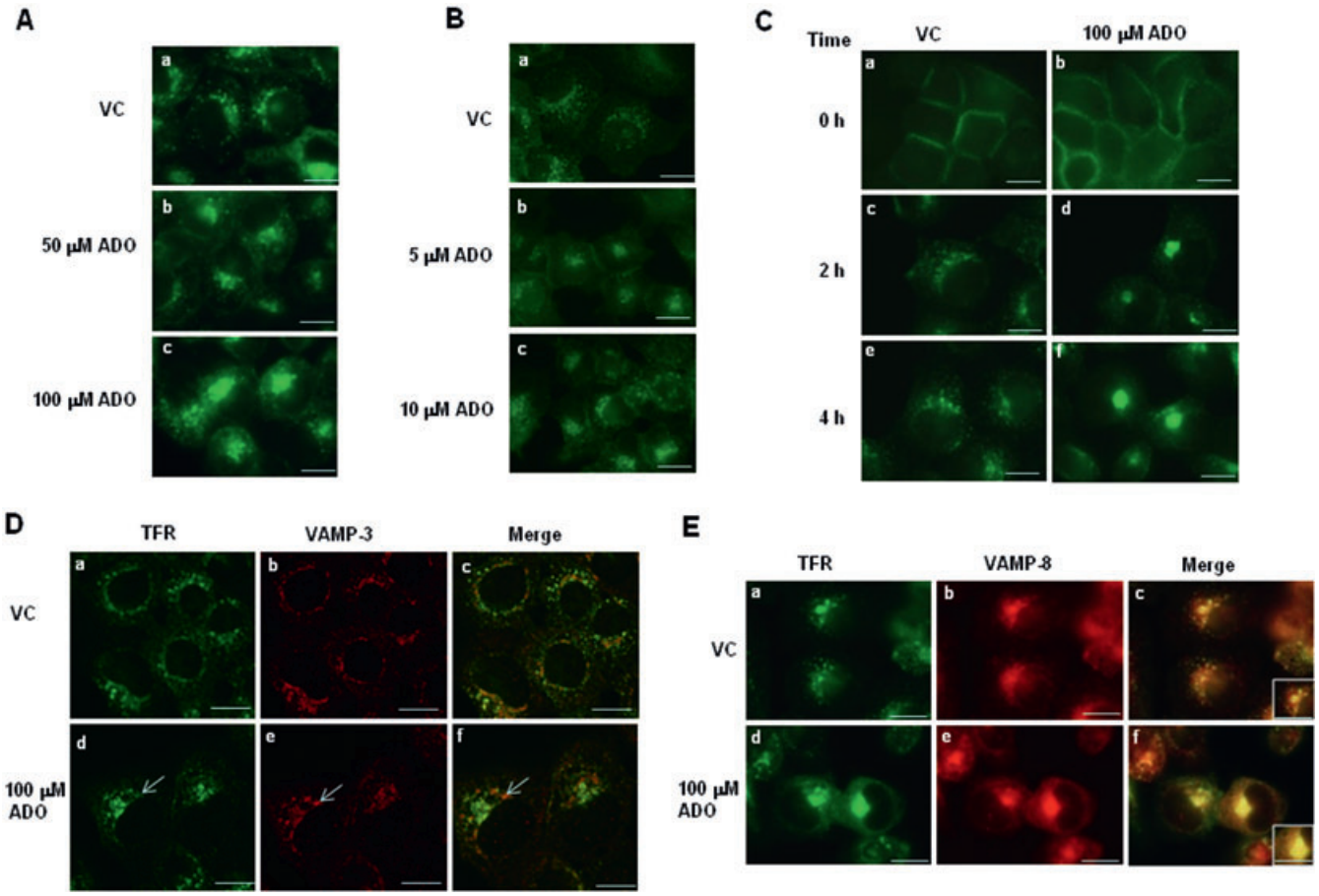

Figure 4 Andrographolide (ADO) affected the intracellular distribution of TfRs. A-431 cells were treated with various concentrations of ADO for 4 h (A), or 24 h (B), then fixed and stained with antibodies; or they were incubated with primary antibody on ice, and then treated with various concentrations of ADO at 37°C, fixed and stained (C, D, E). Primary antibodies used were against TfR (monoclonal), VAMP-3 (polyclonal), and VAMP-8 (polyclonal), and secondary antibodies were FITC-conjugated anti-mouse IgG and Cy-3 conjugated anti-rabbit IgG. Photos are representative of at least two independent experiments, and were taken with the Olympus BX60 (A, B, C, E) and Leica TS5 confocal microscope (D) at 100× magnification. Scale bars represent 10 μm. (A) Effect of andrographolide on steady state TfRs after the 4 h treatment. (B) Effect of andrographolide on steady state TfRs after the 24 h treatment. (C) Effect of andrographolide on TfRs internalized from the cell surface. The time points tested were 2 h and 4 h. (D) The perinuclear clump of TfRs did not co-localize well with VAMP-3. (E) The perinuclear clump of TfRs co-localized well with VAMP-8. Inset image shows enlarged image of TfR, VAMP-8 co-localization. EGFR, epidermal growth factor receptor; TfR, transferrin receptor; VAMP, vesicle-associated membrane protein; VC, vehicle control.

with acid solution to remove anti-EGFR antibody remaining on the cell surface. Cells were then fixed and stained with FITC-conjugated secondary antibodies and the amount of intracellular anti-EGFR antibody was quantified by flow-cytometry. Interestingly, andrographolide was found to enhance the rate of EGFR internalization from the cell surface (Figure 6A, b). Therefore, the increase in the rate of internalization of EGFRs accounts for the decrease in the number of surface EGFRs after andrographolide treatment. This effect was specific for EGFRs, as andrographolide did not significantly enhance internalization of TfRs from the cell surface (Figure 6A, c)

From the above result, it was of interest to find out if andrographolide could induce phosphorylation of EGFRs so as to increase the internalization rate, as activated EGFRs are known to be endocytosed. Cells deprived of serum were treated in two separate groups – one group was pretreated with andrographolide for 4 h, the other group was induced with EGF for 15 min. Both groups were then detached and lysed and analysed by Western blot for activated EGFRs. Andrographolide was unable to induce the phosphorylation of EGFRs (Figure 6B).

Discussion

Thus far, no work has been carried out to determine if andrographolide modulates receptor trafficking, particularly receptors that are implicated in cancer progression like EGFRs and those important for cell survival like TfRs. Here, we demonstrated that andrographolide can affect receptor trafficking. Although the concentration of andrographolide utilized in this study is higher than that used in most other studies, the effect of andrographolide observed on A-431 cells at 100 μM for 4 h similarly occurs at 5 μM or 10 μM after 24 h of treatment. We also observed down-regulation of close to 30% of cell surface EGFRs after treatment with 5 μM andrographolide for 48 h (Figure 1C), as well as the formation of the PCM for

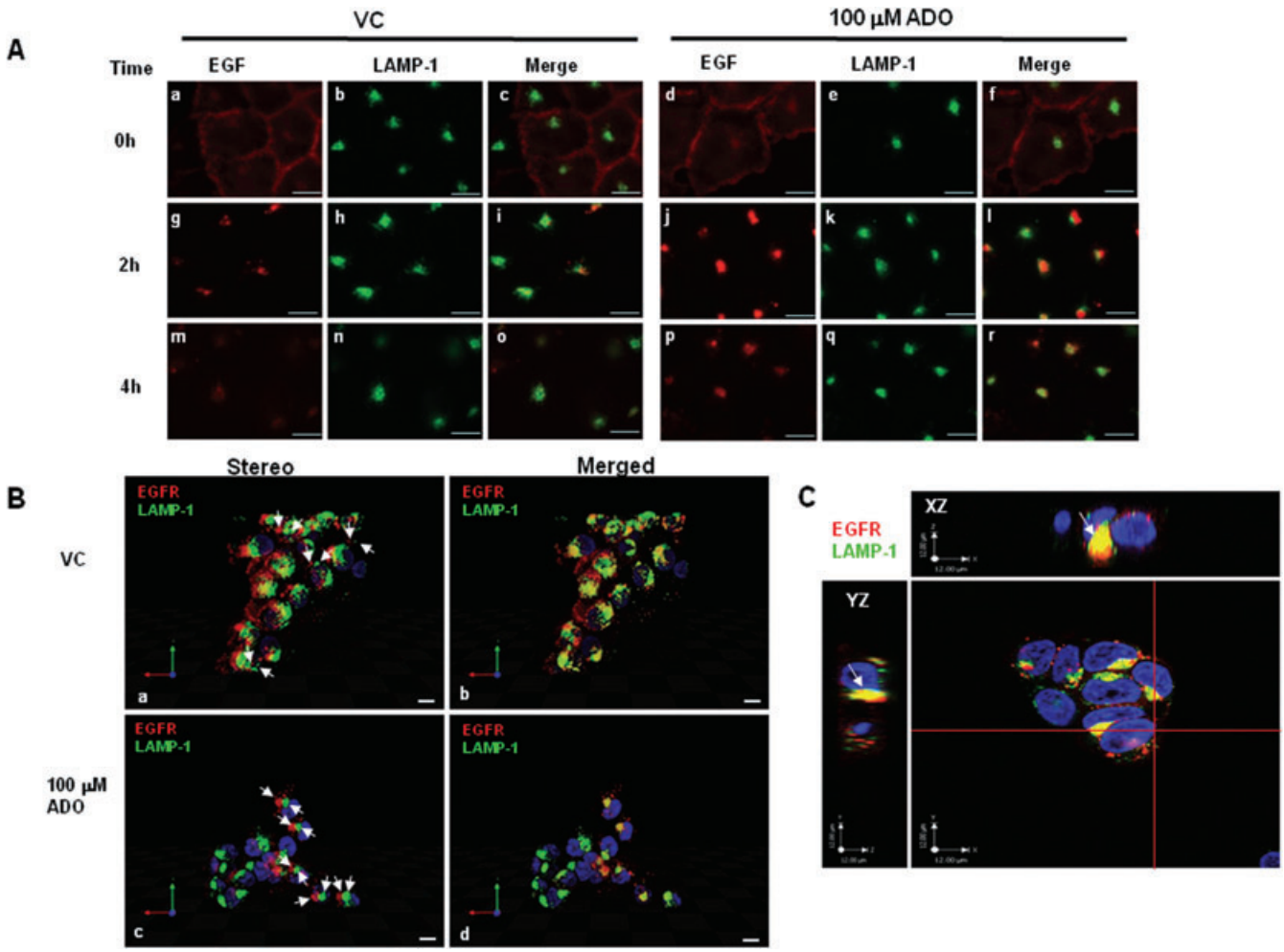

Figure 5 Epidermal growth factor receptor (EGFR) accumulated in an intracellular membrane compartment that co-localizes with LAMP-1 upon treatment with andrographolide (ADO). Cells were incubated with labelled EGF on ice, treated with various concentrations of ADO, then fixed and stained with antibody against LAMP-1 (monoclonal). Photos are representative of at least two independent experiments. (A) Internalized labelled EGF co-localized with LAMP-1. The time points tested were 2 h and 4 h. Images were taken using Olympus BX60. Scale bars represent 10 μm. (B) Stereo three-dimensional convolution image of EGF co-localization with LAMP-1. Images were taken using the confocal microscope Olympus Fluoview 500. Stereo three-dimensional rendering was performed using the volocity visualization software from Improvision. Scale bar represents 5 μm. (C) X-Z/Y-Z projection of EGF co-localization with LAMP-1. Images were taken using Olympus Fluoview 500. X-Z/Y-Z projection was performed using the volocity visualization software from Improvision. Scale bar represents 12 μm. LAMP-1, lysosomal-associated membrane protein-1.

EGFR and TfR after treatment with 5 μM and 10 μM for 24 h (Figures 3B and 4B). Thus, it is possible that the effect of andrographolide at a higher concentration for a shorter incubation time is similar to the effect of a lower concentration for a longer incubation time. We chose to work with a shorter time point and a higher concentration to ensure that the observed effects on receptor trafficking were not downstream events of cells dying due to long hours of drug treatment. The effects of 10 μM andrographolide on EGFR and TfR after 24 h are comparable to other studies; a similar concentration of andrographolide was utilized on human colorectal carcinoma Lovo cells to inhibit cell growth (Shi *et al.*, 2008), and 50 μM andrographolide for 24 h was used to induce apoptosis in Hela and HepG2 cells (Zhou *et al.*, 2006). Hence, the effects of andrographolide on receptor trafficking are most probably events that are not downstream effects of cell death.

Comparisons of the effective concentrations on EGFR and TfR at 24 h to those found in *in vivo* pharmacokinetics studies using normal therapeutic doses reveal that it may be necessary to use higher doses of andrographolide to induce an anticancer effect *in vivo*. Plasma concentrations of andrographolide in humans treated with Kan Jang at a daily therapeutic dosage of 1 mg ADO·kg^{-1} body weight·day^{-1}, which is approximately 60 mg of andrographolide, peaked at 3.8 μM (Panossian *et al.*, 2000), which is slightly lower than the effective concentrations of 5 and 10 μM. It is possible to attain much higher plasma concentrations by administering a higher dose, as preliminary pharmacokinetic studies in mice treated with 150 mg ADO·kg^{-1} have been found to yield maximal plasma concentrations of 20–30 μM (Stanslas *et al.*, 2001) However, in the process of dosage optimization to achieve the anticancer effect of andrographolide, it is important to bear in mind results from previous clinical trials and toxicity tests. The LD_{50} of andrographolide in mice was found to be more than 4000 mg ADO·kg^{-1}·day^{-1} (Chen *et al.*, 2009), while a small clinical trial conducted in both HIV positive and

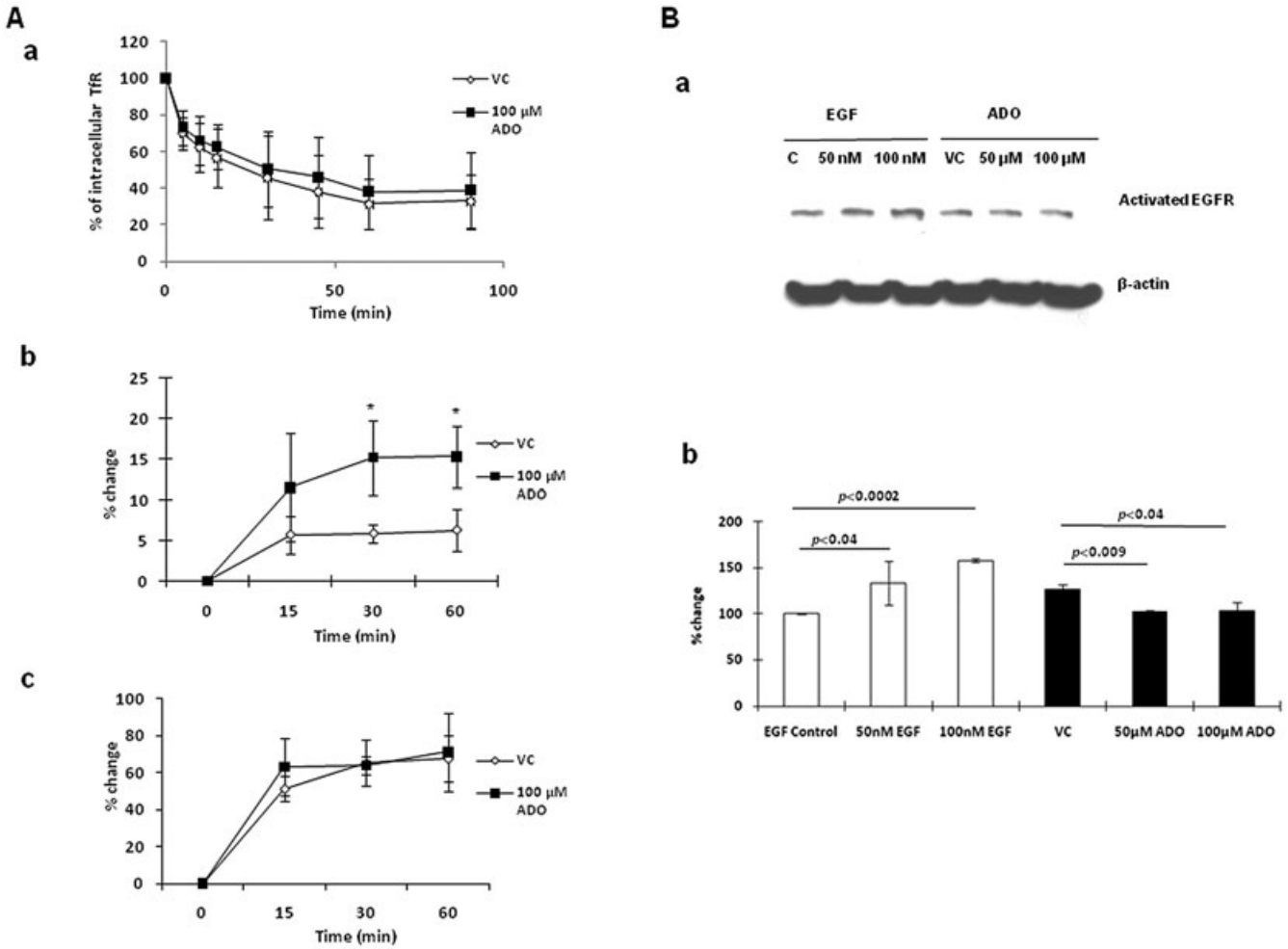

Figure 6 Andrographolide (ADO) did not affect the recycling pathway, but increased the internalization of EGFR. (A) (a) A-431 cells were pretreated with DMSO or 100 μM ADO for 4 h in serum-free DMEM, and then incubated with Alexa Fluor 488 labelled transferrin at 17°C. Unbound transferrin was then washed off and internalized transferrin allowed to recycle for 0–90 min. The amount of unrecycled transferrin in the cells was quantified and expressed as a percentage of total bound transferrin. Results are expressed as a mean percentage ± SD from two independent experiments. (b) ADO increased the internalization of EGFR. A-431 cells were pretreated with DMSO or 100 μM ADO for 4 h, and then incubated with anti-EGFR on ice for 1 h, before being placed in media and fixed at various time points. Cells were then stained with FITC-conjugated anti mouse IgG and read with the flow cytometer. Results are expressed as a percentage of the total amount of EGFR on the cell surface ± SD from two independent experiments. (c) ADO did not increase the internalization of TfR. A-431 cells were pretreated with DMSO or 100 μM ADO for 4 h, and then incubated with anti-TfR on ice for 1 h, before being placed in the media and fixed at various time points. Cells were then stained with FITC-conjugated anti-mouse IgG and read with the flow cytometer. Results are expressed as a percentage of the total amount of TfR on the cell surface ± SD from two independent experiments. (B) ADO did not induce the phosphorylation of EGFR. For the EGF group, A-431 cells were deprived of serum and then treated with various concentrations of EGF for 15 min. For the ADO group, A-431 cells were deprived of serum and treated with DMSO or ADO for 4 h, then lysed and used for Western blot analysis. Blots were probed for activated EGFR; β-actin was the loading control. The intensity of the activated EGFR bands was quantified, normalized to β-actin bands, and expressed as a percentage of the control ± SD of at least two experiments. Blots are representative of at least two experiments. (a) Western blot of phosphorylated EGFR. (b) Quantification of phosphorylated EGFR. EGFR, epidermal growth factor receptor; TfR, transferrin receptor.

negative volunteers utilizing higher doses of 5 mg ADO·kg^{-1} body weight and 10 mg ADO·kg^{-1} body weight, administered three times a day, to test for toxicity did show some adverse effects in the form of a rash and diarrhoea, but the levels of the liver enzymes, aspartate transaminase (AST) and alanine transaminase (ALT), were not significantly affected in normal subjects during the medication period (Calabrese *et al.*, 2000). Hence, an optimum dose within the range of 60 mg to 300 mg·day^{-1} could be used to achieve the anticancer effects of andrographolide in humans without any adverse effects.

Here, we have demonstrated that andrographolide down-regulates cell surface EGFR and also slows down the degradation of both EGFR and TfR, causing them to accumulate in the late endosomes (Figure 7). After andrographolide treatment, upon activation with their ligand, EGFR self-phosphorylate and are internalized at an increased rate from the cell surface (Figure 6A, b), where they move into the early endosomes and progress to the late endosomes. Interestingly, from our observations, the down-regulation of cell surface EGFR is not dose-dependent (Figure 1B). It is possible that the effect of andrographolide on the trafficking machinery involved in internalizing cell surface EGFR is saturated at 50 μM for 4 h and 5 μM for 48 h. In the presence of andrographolide, the degradation of EGFR is slowed down such that it accumulates

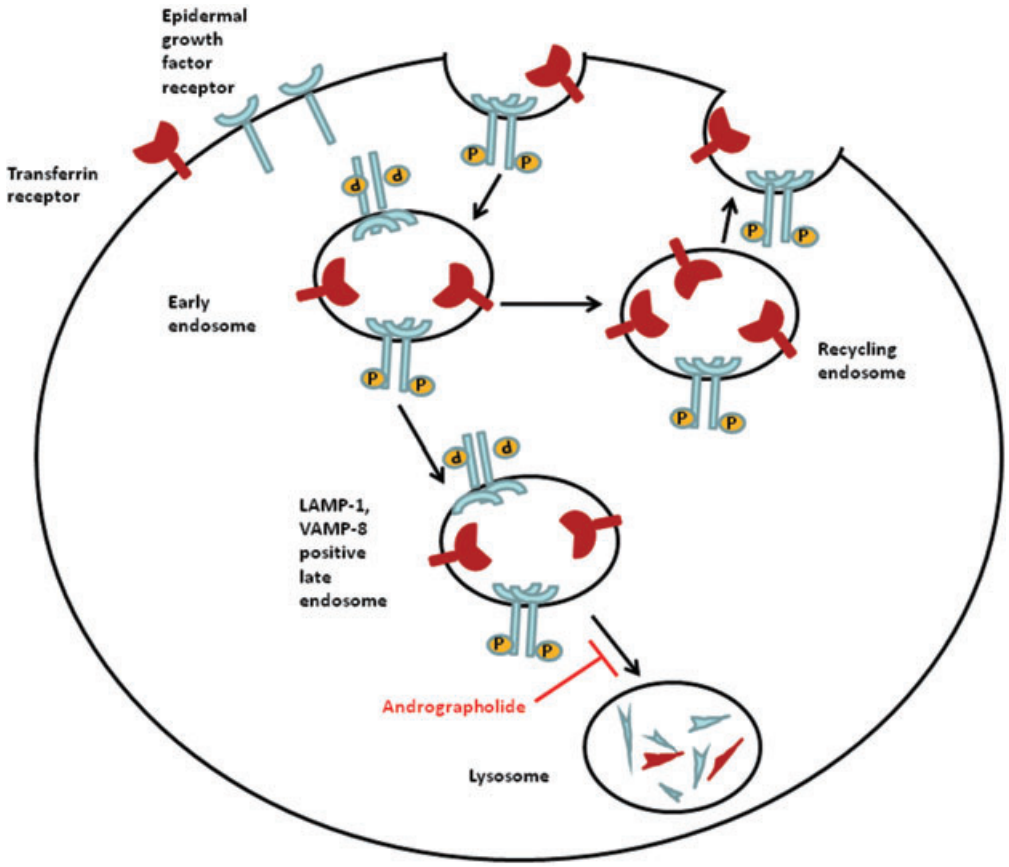

Figure 7 Proposed mechanism of andrographolide (ADO)-induced inhibition of receptor degradation in late endosomes monomeric EGFR dimerizes upon binding of a ligand, following which the tyrosine kinases autophosphorylate, and enter the cell by endocytosis. Similarly, TfR enters the cell by endocytosis constitutively, and a portion of both EGFR and TfR receptors are recycled back to the surface. Receptor trafficking from the late endosome to the lysosome is inhibited after ADO treatment. EGFR, epidermal growth factor receptor; TfR, transferrin receptor.

in the VAMP-8 positive compartment. Similarly, TfR constitutively internalizes from the cell surface, where it either enters the recycling endosomes to travel back to the plasma membrane, or it enters the late endosomes. In the presence of andrographolide, similar to EGFR, on entry to the late endosomes, it also accumulates in a VAMP-8 positive compartment (Figure 7). It can be inferred that the VAMP-8 and LAMP-1 positive compartment that EGFRs are accumulated in is the late endosomal compartment, as VAMP-8 is known to be found in both early and late endosomes (Antonin *et al.*, 2000), whereas LAMP-1 is expressed in both the late endosomes and lysosomes (Eskelinen *et al.*, 2003). The accumulation of EGFRs in the late endosome is expected as, after being internalized, the EGFR traffics rapidly from the cell surface into the late endosomes for degradation. Here, we propose that andrographolide acts in two ways to cause the accumulation of receptors: it increases the internalization rate of EGFRs from the cell surface and, also, inhibits their degradation by reducing their movement into the lysosomes from late endosomes. The increase in internalization rate is not the only reason for receptor accumulation as the TfRs did not internalize more rapidly after andrographolide treatment, but their degradation was inhibited. Hence, the inhibition in the movement of receptors into the lysosomes is more likely to be a greater contributor. In addition, we have also ruled out the possibility that andrographolide inhibits some lysosomal enzymes after treatment for 4 h (data not shown), although it is possible that the endosomal sorting complex required for transport (ESCRT) machinery, which is responsible for receptor down-regulation induced by trafficking receptors from the endosomes/multivesicular bodies to the lysosomes (Kirisits *et al.*, 2007; Saksena and Emr, 2009), is affected by andrographolide. Both EGFR and TfR also differ at the time point where the accumulation of receptors is obvious (Figure 2). This most likely due to the difference in the pathways in EGFR and TfR; EGFR is delivered directly for degradation after internalization, whereas a large pool of TfRs undergoes a few rounds of recycling to the cell surface before being sent for degradation (Daniels *et al.*, 2006). Hence, it would take a longer time for the accumulation of TfRs to be noticed. The accumulation of TfRs was also more distinct as it took longer for them to be degraded, hence the cells could be treated for 6 h.

The inhibition of protein trafficking to the lysosome for degradation is detrimental to cell survival (Figure 1A). Lysosomes are acidic, hydrolase-containing organelles in the cell responsible for protein degradation and recycling (Eskelinen *et al.*, 2003), and proteins are trafficked to lysosomes either from autophagosomes or late endosomes (Nixon *et al.*, 2008). Failure to break down proteins targeted for degradation

efficiently is known to be associated with the disruption of cellular function. Recently, it was shown that the inhibition of rhodopsin trafficking to lysosomes resulted in its accumulation in late endosomes. This accumulation caused the death of photoreceptor cells, leading to blindness (Chinchore *et al.*, 2009). Hence, inhibiting protein trafficking to the lysosome is a possible mechanism by which andrographolide could induce cell death.

It may also seem paradoxical that andrographolide inhibits cell growth despite inducing the accumulation of internalized EGFR (Figure 2), as lysosomal degradation is thought to be one of the modes of down-regulating EGFR-mediated signalling. However, it has been demonstrated in MDA-MB-468 breast cancer cells, which overexpress EGFRs, that internalized EGFRs are capable of activating caspase-3 to induce cell death (Hyatt and Ceresa, 2008). As A-431 is known to express caspase-3 (Mese *et al.*, 2000), it is possible that the accumulation of EGFRs in the late endosomes induced by andrographolide may then result in cell death by the activation of caspase-3.

Finally, the down-regulation of surface EGFRs induced by andrographolide (Figure 1B), caused by the increased rate of internalization of receptors (Figure 6A, b), is also another mechanism by which andrographolide could induce cell death. Previously, it was demonstrated that knockdown of EGFR by siRNA in human glioma cells resulted in a decrease in cell survival (Kang *et al.*, 2005). This is expected as EGFR is also a receptor that is known to be upstream of the mitogen-associated protein kinase (MAPK) and phosphatidylinositol 3-kinase (PI3K) signalling cascades that control cell proliferation (Hynes and Lane, 2005), and thus down-regulation of surface EGFR could inhibit tumour proliferation in the presence of growth factors.

Currently, there are two main classes of anticancer agents targeting EGFR (Hynes and Lane, 2005; Zhang *et al.*, 2007). The first class is made up of monoclonal antibodies such as cetuximab and panitumumab, which target the extracellular domain of EGFR to inhibit ligand binding. Reversible and irreversible tyrosine kinase inhibitors such as gefitinib and erlotinib form the second class, and they inhibit the activation of EGFR, and hence the downstream cell proliferation, signalling pathways (Yap *et al.*, 2009; Zahorowska *et al.*, 2009). We have shown here for the first time that andrographolide, a small chemical compound which does not belong to these two classes of anticancer agents, can be used to target EGFR. Another emerging small molecule in the area of anticancer therapy is the major catechin found in green tea (–)-epigallocatechin gallate (EGCG) (Yang *et al.*, 2009a). EGCG has not only been found to inhibit activation of EGFR and its downstream signalling pathways (Shimizu *et al.*, 2008), but it is also capable of down-regulating EGFR by inducing its internalization (Adachi *et al.*, 2008). However, in contrast to andrographolide, EGFRs internalized after EGCG treatment are recycled to the cell surface after removal of EGCG. Hence, the ability of andrographolide to increase the internalization of cell surface EGFRs and cause them to accumulate in the late endosomes is unique.

Andrographolide has been shown previously to have anticancer properties; it induces cell cycle arrest at the G2/M phase in HepG2 cells (Li *et al.*, 2007), and at the G0/G1 phase in HL-60 leukaemic cells (Cheung *et al.*, 2005). It can also induce apoptosis in cancer cells in a caspase-3 (Zhao *et al.*, 2008) and -8 dependent manner (Zhou *et al.*, 2006) as well as inhibit NF-κB binding of DNA by forming a covalent bond with the reduced 62 cysteine of p50 (Xia *et al.*, 2004; Hidalgo *et al.*, 2005). The immunosuppressive ability of andrographolide through its effect on NF-κB would be a useful property in an anticancer drug, especially as NF-κB has, in recent years, emerged as a target for cancer therapy (Baud and Karin, 2009). For example, NF-κB activation has been implicated in cancers such as breast, colon, liver, prostate, cervical and acute lymphocytic leukaemia, and its prolonged activation results in increased cell survival and proliferation, tumour metastasis and angiogenesis, factors which are involved in cancer progression (Baud and Karin, 2009). Our work on EGFR and TfR here has added a new dimension to the utilization of andrographolide as an anticancer drug, as well as provided an understanding into how andrographolide regulates receptor trafficking in the cell.

Acknowledgements

This work was supported by research grants from the Academic Research Council-Ministry of Education, Singapore (R182-000-099-112 to W.S.H.) and the Singapore National Medical Research Council (R182-000-137-213 to W.S.H.).

Conflict of interest

None.

References

Adachi S, Nagao T, To S, Joe AK, Shimizu M, Matsushima-Nishiwaki R *et al.* (2008). (-)-Epigallocatechin gallate causes internalization of the epidermal growth factor receptor in human colon cancer cells. *Carcinogenesis* **29**: 1986–1993.

Alexander SP, Mathie A, Peters JA (2008). Guide to Receptors and Channels (GRAC), 3rd edition. *Br J Pharmacol* **153** (Suppl. 2): S1–S209.

Antonin W, Holroyd C, Tikkanen R, Honing S, Jahn R (2000). The R-SNARE endobrevin/VAMP-8 mediates homotypic fusion of early endosomes and late endosomes. *Mol Biol Cell* **11**: 3289–3298.

Bao Z, Guan S, Cheng C, Wu S, Wong SH, Kemeny DM *et al.* (2009). A novel antiinflammatory role for andrographolide in asthma via inhibition of the nuclear factor-kappaB pathway. *Am J Respir Crit Care Med* **179**: 657–665.

Baud V, Karin M (2009). Is NF-kappaB a good target for cancer therapy? Hopes and pitfalls. *Nat Rev Drug Discov* **8**: 33–40.

Calabrese C, Berman SH, Babish JG, Ma X, Shinto L, Dorr M *et al.* (2000). A phase I trial of andrographolide in HIV positive patients and normal volunteers. *Phytother Res* **14**: 333–338.

Capdevila J, Elez E, Macarulla T, Ramos FJ, Ruiz-Echarri M, Tabernero J (2009). Anti-epidermal growth factor receptor monoclonal antibodies in cancer treatment. *Cancer Treat Rev* **35**: 354–363.

Chen JX, Xue HJ, Ye WC, Fang BH, Liu YH, Yuan SH *et al.* (2009). Activity of andrographolide and its derivatives against influenza virus in vivo and in vitro. *Biol Pharm Bull* **32**: 1385–1391.

Cheung HY, Cheung SH, Li J, Cheung CS, Lai WP, Fong WF *et al.*

(2005). Andrographolide isolated from Andrographis paniculata induces cell cycle arrest and mitochondrial-mediated apoptosis in human leukemic HL-60 cells. *Planta Med* **71**: 1106–1111.

Chinchore Y, Mitra A, Dolph PJ (2009). Accumulation of rhodopsin in late endosomes triggers photoreceptor cell degeneration. *Plos Genet* **5**: e1000377.

Daniels TR, Delgado T, Rodriguez JA, Helguera G, Penichet ML (2006). The transferrin receptor part I: Biology and targeting with cytotoxic antibodies for the treatment of cancer. *Clin Immunol* **121**: 144–158.

Dy GK, Adjei AA (2009). Emerging therapeutic targets in non-small cell lung cancer. *Proc Am Thorac Soc* **6**: 218–223.

Eskelinen EL, Tanaka Y, Saftig P (2003). At the acidic edge: emerging functions for lysosomal membrane proteins. *Trends Cell Biol* **13**: 137–145.

Goding JW, Burns GF (1981). Monoclonal antibody OKT-9 recognizes the receptor for transferrin on human acute lymphocytic leukemia cells. *J Immunol* **127**: 1256–1258.

Gold KA, Lee HY, Kim ES (2009). Targeted therapies in squamous cell carcinoma of the head and neck. *Cancer* **115**: 922–935.

Habashy HO, Powe DG, Staka CM, Rakha EA, Ball G, Green AR *et al*. (2010). Transferrin receptor (CD71) is a marker of poor prognosis in breast cancer and can predict response to tamoxifen. *Breast Cancer Res Treat* **119**: 283–293.

Hidalgo MA, Romero A, Figueroa J, Cortes P, Concha II, Hancke, JL, Burgos RA (2005). Andrographolide interferes with binding of nuclear factor-kappaB to DNA in HL-60-derived neutrophilic cells. *Br J Pharmacol* **144**: 680–686.

Hong W (2005). SNAREs and traffic. *Biochim Biophys Acta* **1744**: 120–144.

Hopkins CR, Trowbridge IS (1983). Internalization and processing of transferrin and the transferrin receptor in human carcinoma A431 cells. *J Cell Biol* **97**: 508–521.

Hyatt DC, Ceresa BP (2008). Cellular localization of the activated EGFR determines its effect on cell growth in MDA-MB-468 cells. *Exp Cell Res* **314**: 3415–3425.

Hynes NE, Lane HA (2005). ERBB receptors and cancer: the complexity of targeted inhibitors. *Nat Rev Cancer* **5**: 341–354.

Iruretagoyena MI, Tobar JA, Gonzalez PA, Sepulveda SE, Figueroa CA, Burgos RA *et al*. (2005). Andrographolide interferes with T cell activation and reduces experimental autoimmune encephalomyelitis in the mouse. *J Pharmacol Exp Ther* **312**: 366–372.

Kang CS, Pu PY, Li YH, Zhang ZY, Qiu MZ, Huang Q *et al*. (2005). An in vitro study on the suppressive effect of glioma cell growth induced by plasmid-based small interference RNA (siRNA) targeting human epidermal growth factor receptor. *J Neurooncol* **74**: 267–273.

Kesari S, Ramakrishna N, Sauvageot C, Stiles CD, Wen PY (2006). Targeted molecular therapy of malignant gliomas. *Curr Oncol Rep* **8**: 58–70.

Kim TG, Hwi KK, Hung CS (2005). Morphological and biochemical changes of andrographolide-induced cell death in human prostatic adenocarcinoma PC-3 cells. *In Vivo* **19**: 551–557.

Kirisits A, Pils D, Krainer M (2007). Epidermal growth factor receptor degradation: an alternative view of oncogenic pathways. *Int J Biochem Cell Biol* **39**: 2173–2182.

Kodama T, Hayasaka S, Setogawa T (1995). Immunohistochemical localization of epidermal growth factor receptor and epithelial antigen in tumors of the human conjunctiva, eyelid, lacrimal gland, and orbit. *Graefes Arch Clin Exp Ophthalmol* **233**: 672–676.

Kumar RA, Sridevi K, Kumar NV, Nanduri S, Rajagopal S (2004). Anticancer and immunostimulatory compounds from Andrographis paniculata. *J Ethnopharmacol* **92**: 291–295.

Lafky JM, Wilken JA, Baron AT, Maihle NJ (2008). Clinical implications of the ErbB/epidermal growth factor (EGF) receptor family and its ligands in ovarian cancer. *Biochim Biophys Acta* **1785**: 232–265.

Le Roy C, Wrana JL (2005). Clathrin- and non-clathrin-mediated endocytic regulation of cell signalling. *Nat Rev Mol Cell Biol* **6**: 112–126.

Lepelletier Y, Camara-Clayette V, Jin H, Hermant A, Coulon S, Dussiot M *et al*. (2007). Prevention of mantle lymphoma tumor establishment by routing transferrin receptor toward lysosomal compartments. *Cancer Res* **67**: 1145–1154.

Li J, Cheung HY, Zhang Z, Chan GK, Fong WF (2007). Andrographolide induces cell cycle arrest at G2/M phase and cell death in HepG2 cells via alteration of reactive oxygen species. *Eur J Pharmacol* **568**: 31–44.

Manikam SD, Stanslas J (2009). Andrographolide inhibits growth of acute promyelocytic leukaemia cells by inducing retinoic acid receptor-independent cell differentiation and apoptosis. *J Pharm Pharmacol* **61**: 69–78.

Maxfield FR, McGraw TE (2004). Endocytic recycling. *Nat Rev Mol Cell Biol* **5**: 121–132.

Mese H, Sasaki A, Nakayama S, Alcalde RE, Matsumura T (2000). The role of caspase family protease, caspase-3 on cisplatin-induced apoptosis in cisplatin-resistant A431 cell line. *Cancer Chemother Pharmacol* **46**: 241–245.

Nixon RA, Yang DS, Lee JH (2008). Neurodegenerative lysosomal disorders: a continuum from development to late age. *Autophagy* **4**: 590–599.

Pannecouque C, Daelemans D, De Clercq E (2008). Tetrazolium-based colorimetric assay for the detection of HIV replication inhibitors: revisited 20 years later. *Nat Protoc* **3**: 427–434.

Panossian A, Hovhannisyan A, Mamikonyan G, Abrahamian H, Hambardzumyan E, Gabrielian E *et al*. (2000). Pharmacokinetic and oral bioavailability of andrographolide from Andrographis paniculata fixed combination Kan Jang in rats and human. *Phytomedicine* **7**: 351–364.

Pike LJ (2005). Growth factor receptors, lipid rafts and caveolae: an evolving story. *Biochim Biophys Acta* **1746**: 260–273.

Rajagopal S, Kumar RA, Deevi DS, Satyanarayana C, Rajagopalan R (2003). Andrographolide, a potential cancer therapeutic agent isolated from Andrographis paniculata. *J Exp Ther Oncol* **3**: 147–158.

Saksena S, Emr SD (2009). ESCRTs and human disease. *Biochem Soc Trans* **37** (Pt 1): 167–172.

Sheeja K, Kuttan G (2006). Protective effect of Andrographis paniculata and andrographolide on cyclophosphamide-induced urothelial toxicity. *Integr Cancer Ther* **5**: 244–251.

Shi MD, Lin HH, Lee YC, Chao JK, Lin RA, Chen JH (2008). Inhibition of cell-cycle progression in human colorectal carcinoma Lovo cells by andrographolide. *Chem Biol Interact* **174**: 201–210.

Shimizu M, Shirakami Y, Moriwaki H (2008). Targeting receptor tyrosine kinases for chemoprevention by green tea catechin, EGCG. *Int J Mol Sci* **9**: 1034–1049.

Singha PK, Roy S, Dey S (2007). Protective activity of andrographolide and arabinogalactan proteins from Andrographis paniculata Nees. against ethanol-induced toxicity in mice. *J Ethnopharmacol* **111**: 13–21.

Stanslas J, Liew PS, Lftlkhar N, Lee CP, Saad S, Lajis N *et al*. (2001). Potential of AG in the treatment of breast cancer. *Eur J Cancer* **37** (Suppl. 6): 169.

Wong SH, Xu Y, Zhang T, Griffiths G, Lowe SL, Subramaniam VN *et al*. (1999). GS32, a novel Golgi SNARE of 32 kDa, interacts preferentially with syntaxin 6. *Mol Biol Cell* **10**: 119–134.

Wong SH, Zhang T, Xu Y, Subramaniam VN, Griffiths G, Hong W (1998). Endobrevin, a novel synaptobrevin/VAMP-like protein preferentially associated with the early endosome. *Mol Biol Cell* **9**: 1549–1563.

Wrann MM, Fox CF (1979). Identification of epidermal growth factor receptors in a hyperproducing human epidermoid carcinoma cell line. *J Biol Chem* **254**: 8083–8086.

Xia YF, Ye BQ, Li YD, Wang JG, He XJ, Lin X *et al*. (2004). Andrographolide attenuates inflammation by inhibition of NF-kappa B activation through covalent modification of reduced cysteine 62 of p50. *J Immunol* **173**: 4207–4217.

Yang CS, Wang X, Lu G, Picinich SC (2009a). Cancer prevention by

tea: animal studies, molecular mechanisms and human relevance. *Nat Rev Cancer* **9**: 429–439.

Yang L, Wu D, Luo K, Wu S, Wu P (2009b). Andrographolide enhances 5-fluorouracil-induced apoptosis via caspase-8-dependent mitochondrial pathway involving p53 participation in hepatocellular carcinoma (SMMC-7721) cells. *Cancer Lett* **276**: 180–188.

Yap TA, Carden CP, Kaye SB (2009). Beyond chemotherapy: targeted therapies in ovarian cancer. *Nat Rev Cancer* **9**: 167–181.

Zahorowska B, Crowe PJ, Yang JL (2009). Combined therapies for cancer: a review of EGFR-targeted monotherapy and combination treatment with other drugs. *J Cancer Res Clin Oncol* **135**: 1137–1148.

Zhang H, Berezov A, Wang Q, Zhang G, Drebin J, Murali R *et al*. (2007). ErbB receptors: from oncogenes to targeted cancer therapies. *J Clin Invest* **117**: 2051–2058.

Zhao F, He EQ, Wang L, Liu K (2008). Anti-tumor activities of andrographolide, a diterpene from Andrographis paniculata, by inducing apoptosis and inhibiting VEGF level. *J Asian Nat Prod Res* **10**: 467–473.

Zhou J, Zhang S, Ong CN, Shen HM (2006). Critical role of pro-apoptotic Bcl-2 family members in andrographolide-induced apoptosis in human cancer cells. *Biochem Pharmacol* **72**: 132–144.

Supporting information

Additional Supporting Information may be found in the online version of this article:

Figure S1 X-Z/Y-Z projection of EGFR withVAMP-3 after andrographolide treatment. A-431 cells were incubated with anti-EGFR on ice, treated with 100 μM andrographolide for 4 h at 37°C, and then fixed and stained with anti-VAMP-3 antibody. Photomicrographs are representative of at least two independent experiments, and were taken with the Olympus FV 1000 at 100× magnification. Scale bars represent 10 μm.

Please note: Wiley-Blackwell are not responsible for the content or functionality of any supporting materials supplied by the authors. Any queries (other than missing material) should be directed to the corresponding author for the article.